05,06

Magnetoelectric effect in hybrid structures metal–magnetoelectric–metal

© N.N. Poddubnaya[1], V.M. Laletin[1], D.A. Filippov[2]

[1] Institute of Technical Acoustics, National Academy of Sciences of Belarus, Vitebsk, Belarus
[2] Novgorod State University, Veliky Novgorod, Russia

E-mail: poddubnaya.n@rambler.ru

Received August 18, 2023
Revised August 18, 2023
Accepted August 23, 2023

To increase magnetoelectric conversion, composite magnetoelectric structures based on a bulk magnetoelectric composite lead zirconate-titanate: nickel ferrite, on which layers of nickel and alternating layers of nickel-cobalt are deposited on both sides by electrochemical deposition, were obtained for the first time. The field dependences of the linear low-frequency magnetoelectric effect of the resulting structures have been studied. It is shown that in hybrid structures the value of the magnetoelectric coefficient is one and a half times greater than its value compared to bulk samples of the same composition. In addition, its maximum shifts to the region of weaker fields for both longitudinal and transverse orientations of the magnetic field.

Keywords: magnetostriction, piezoelectricity, magnetoelectric effect, magnetoelectric coefficient, compositional structure.

DOI: 10.61011/PSS.2023.10.57220.184

1. Introduction

Magnetoelectric (ME) composites are among the promising materials for use in straintronics devices — a new direction in electronics [1]. On their basis it is possible, in particular, to create such devices as: highly sensitive magnetic field detectors [2–8], energy-harvesters [9], current-voltage converters (gyrators) [10,11], inductors in which the parameters are controlled by both magnetic and electric fields [12]. To obtain the maximum effect the question of increasing the efficiency of the ME conversion remains fundamental, especially in the low-frequency region, where the value of the ME coupling is practically independent of frequency. For this reason, studies continues aimed at obtaining new crystalline and composite structures with high magnetoelectric properties. Many papers relate to studying the properties of bulk materials [13–15], lamellar composites obtained using various technologies [16–20]. A number of papers relate to the study of structures with a polymer matrix [21–23]. There are structures that make it possible to increase the magnitude of the magnetoelectric interaction due to the toroidal shape [24,25] and other complex structures [26]. In this paper we were the first to obtain and study structures with a hybrid type of coupling 2/3–0/2, combining the advantages of both lamellar and bulk composites. The paper was based on the assumption that the ME transformation is enhanced due to increase in the magnetic field acting on the bulk composite (coupling 3–0) when using ferromagnetic layers in the compositional structure (coupling 2) as magnetic field concentrators [27], as well as increase in the deformations of the piezoelectric phase due to the additional contribution from the magnetostrictive layers.

2. Materials and methods

A bulk composite magnetoelectric material with coupling 3–0 was made from piezoceramic powder of plumbum zirconate titanate PZT 23 (PZT) and magnetostrictive nickel ferrite $NiFe_{1.98}Co_{0.02}O_4$ (NFO). The required composition of nickel ferrite was obtained by double high-temperature synthesis of dehydrated powders NiO, Fe_2O_3 and Co_2O_3. The composition of the charge was calculated taking into account the content of the main substance. The powders were mixed in a jasper mortar in the presence of ethyl alcohol for 30 min. The resulting mixtures were pressed under a pressure of 50 MPa using an aqueous solution of polyvinyl alcohol (PVA) as a plasticizer. The synthesis was carried out in air at a temperature of 1050°C for two hours. The synthesized ferrite was crushed and ground in the jasper mortar, briquetted again with the addition of PVA, and synthesized at temperature of 1050°C for two hours. The synthesized and ground ferrite powder was sieved through a sieve № 007.

Bulk composites from mixture of piezoceramics and nickel ferrite powders (PZT:NFO) were produced in a similar way. The samples were sintered in crucibles with plumbum-containing backfill for two hours at temperature 1240°C. The manufactured samples had a diameter of 8.7–8.8 mm and were brought to a thickness of 0.4 mm by step-by-step polishing. A nickel sublayer was applied to the samples using chemical metallization from a nickel chloride solution. This sublayer served as electrodes during the subsequent electrochemical deposition of ferromagnetic metals. The resulting compositional structure was polarized normal to the plane in electric field 0.7–4 kV/cm (depending on the composition) in silicone oil. To produce hybrid

structures (2/3–0/2) on bulk PZT:NFO composite, nickel or alternating layers of nickel/cobalt/nickel were deposited on both sides by electrochemical deposition from solutions of nickel sulfamate and cobalt sulfate. The choice of the pair of materials PZT:NFO — nickel was due to the fact that they both have negative magnetostriction and approximately the same values of magnetic fields at which magnetostriction saturation occurs, and the value of saturation magnetostriction, which are respectively equal for nickel [28] to $H_S^{\mathrm{Ni}} = 80\,\mathrm{kA/m}$ and $\lambda_S^{\mathrm{Ni}} = -30\,\mathrm{ppm}$ and for nickel ferrite [29] to $H_S^{\mathrm{NFO}} = 40\,\mathrm{kA/m}$ and $\lambda_S^{\mathrm{NFO}} = -27\,\mathrm{ppm}$. Ni/Co/Ni hybrid structures were used to create a magnetization gradient, which should lead to increase in the effect at zero bias field [30]. The metal layers were deposited using a reversive current with density of $3.5\,\mathrm{A/dm^2}$ with pulse width corresponding to the deposition/dissolution polarity of 90/9 s. The thickness of the layers for different samples was $20-100\,\mu\mathrm{m}$ on each side. The resulting layers represented, in addition to the nickel ferrite in the bulk PZT:NFO composite, a magnetostrictive component with coupling 2 as part of the hybrid structure.

To qualitatively analyze the composition of the resulting structures, we used fracture microstructure studies and chemical elemental analysis performed with a HITACHI S-4800 scanning electron microscope. X-ray diffraction analysis was carried out using a DRON-2 diffraction refractometer. The linear magnetoelectric effect was studied by measuring the voltage arising on the sample under the influence of alternating (H_{ac}) and biasing (H_{bias}) magnetic fields. The alternating magnetic field was created by a Helmholtz coil and its intensity was about $H_{\mathrm{ac}} \sim 80\,\mathrm{A/m}$ at frequency of 1 kHz. The magnetizing field strength varied within $H_{\mathrm{bias}} = -200 - +200\,\mathrm{kA/m}$. The value of ME voltage coefficient α_E was determined using the following relationship:

$$\alpha_E = \left(\frac{V}{t^{ME} H_{\mathrm{ac}}}\right), \qquad (1)$$

where t^{ME} — thickness of the layer of bulk PZT:NFO composite.

3. Results and their discussion

The X-ray diffraction analysis data of the compositional structures of PZT:NFO composition are presented in Figure 1.

The magnitude of the intensity peaks corresponding to scattering angles of 39 and 45°, related to characteristic peaks for PZT ceramics and nickel ferrite, is redistributed in accordance with the change in the initial composition of the ceramic substrate from 90 to 50%° in proportion to the concentration of phases, included in the composite. At the same time, no new compounds or complexes appear in a two-phase solution.

The results of energy dispersive analysis showed a redistribution of characteristic intensity peaks of the main elements in proportion to the concentration of the phases

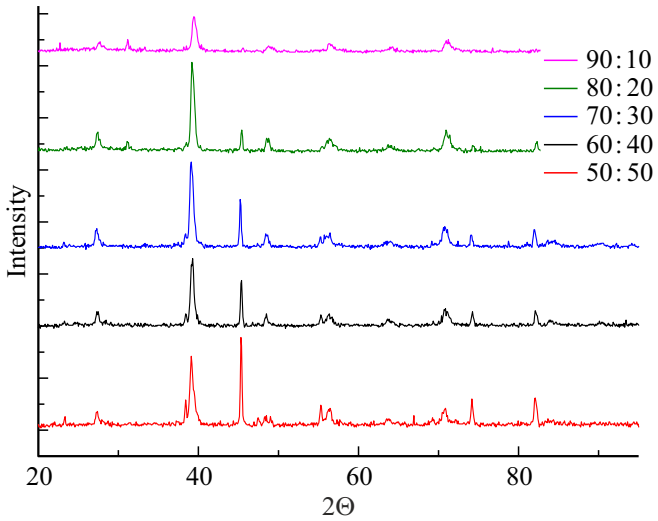

Figure 1. X-ray patterns of bulk compositional structures with different mass ratios PZT:NFO.

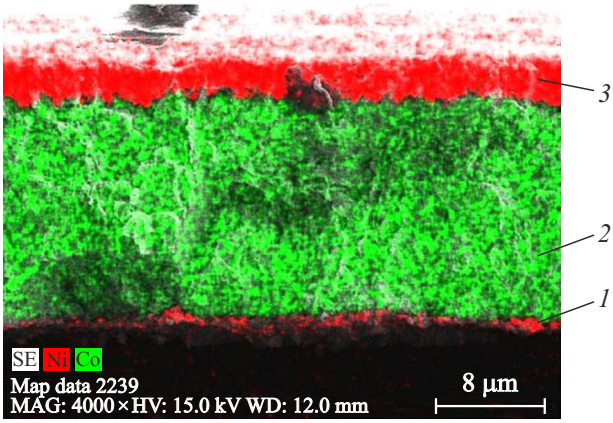

Figure 2. Surface microstructure and energy dispersive analysis of chemical composition of fractured sample. *1* — chemically deposited nickel sublayer, *2* — electrochemically deposited cobalt layer, *3* — electrochemically deposited nickel layer.

included in the composite. Analysis of the chemical elements distribution over the fracture surface in the compositions showed a slight decrease in the uniformity of phases distribution with increase in the relative proportion of ferrite in the composite. In this case, the elemental chemical composition of the samples is preserved, and the change in the concentration of elements in the composition corresponds to the change in the concentration of the ferrite:piezoceramics phases.

The surface elemental composition and fracture microstructure of metal layers were studied for coatings separated from the bulk NFO:PZT composite. The thickness of the chemically deposited nickel sublayer in all cases was less than $1\,\mu\mathrm{m}$ (Figure 2). Nickel particles penetrate into the bulk NFO:PZT composite to a depth of several microns. The study of fractures of various structures showed that the elemental composition of the coatings is maintained for each

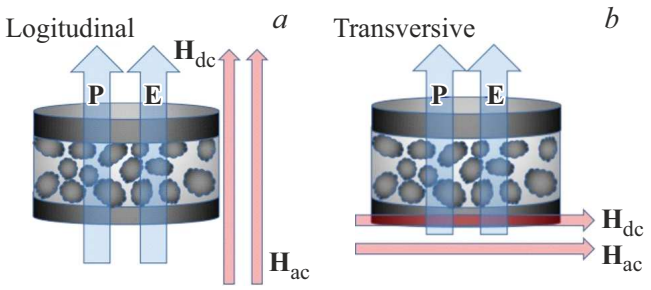

Figure 3. Schematic representation of magnetic fields orientation with respect to the direction of structure polarization: *a* — longitudinal effect, *b* — transverse effect.

solution used and does not depend on the thickness of the coatings.

In experimental study of the low-frequency field dependence of ME voltage coefficient (MEVC) α_E of hybrid structures under the influence of magnetic field the orientations of the magnetic field were used, directed both along the direction of polarization of the structure — longitudinal effect, and perpendicular — transverse effect. A schematic representation of the hybrid structure of the composite and the orientation of polarization and of external magnetic field during study are shown in Figure 3.

In order to identify the contribution of additional magnetostrictive layers to the magnitude of the ME effect, the field dependence of MEVC on the percentage of ferrite in the bulk PZT:NFO composite was first studied. The study results for longitudinal and transverse effects are presented in Figure 4.

The field dependence of MEVC on the percentage of ferrite has a typical dependence [31]. As can be seen from the graphs, the dependences of MEVC on the percentage of ferrite in the composite have maxima, the values of which are observed at approximately equal ratio of NFO and PZT in the composite. With a further increase in ferrite content, the magnitude of the effect decreases. This is due to the fact that in bulk PZT:NFO composite, MEVC value is proportional to the product of the effective values of the piezoelectric and magnetic piezoelectric moduli by the Young's modulus of the composite, and is inversely proportional to the effective dielectric constant [32]. As the percentage content of ferrite increases, the piezoelectric modulus and effective dielectric constant decrease. At the same time, there is increase in the effective piezomagnetic modulus and the effective Young's modulus of the composite. All this leads to the appearance of a maximum in the MEVC dependence on the percentage content of ferrite. It should be noted that the maximum MEVC value is achieved with longitudinal effect in fields near 100 kA/m, while at the transverse effect — in fields near 50 kA/m. Moreover, the higher the ferrite concentration is, the larger the fields are needed to achieve the maximum MEVC value for the longitudinal effect, and the smaller the fields are needed in the case of the transverse effect. This is explained by the magnitude of demagnetizing factors. In bulk and layerd composites the longitudinal effect is significantly less in magnitude then the transverse effect. The magnitude of the longitudinal and transverse effects is comparable in value, which is typical for hybrid structures. In the case of longitudinal orientation of the hybrid composite, the external magnetic field acting on the coupling composite 3–0 is significantly increased due to the magnetic coatings of coupling 2, oriented perpendicular to the induction lines of the external magnetic field. With transverse orientation the magnetic induction lines have almost no such effect, being located in the plane of the magnetic films. This behavior is explained precisely by the structure of the composite 2/3–0/2, polarized perpendicular to the plane of the layers.

To clarify the effect of additional magnetostrictive layers on the bulk PZT:NFO composite, layers of nickel and alternating layers of nickel/cobalt/nickel by electrochemical

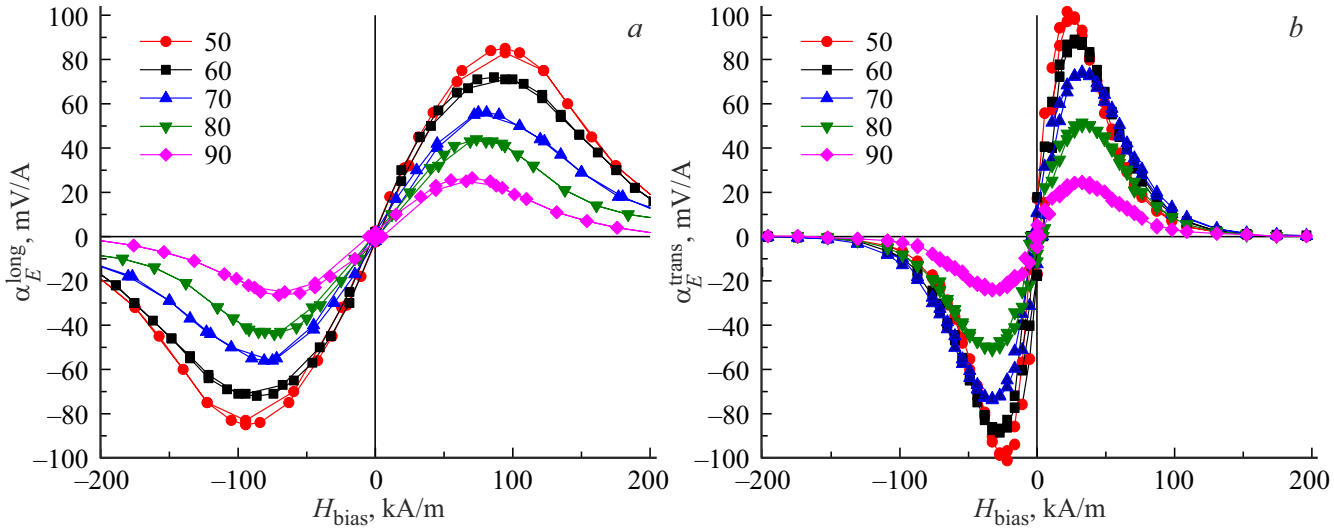

Figure 4. MEVC vs. magnitude of bias field: *a* — longitudinal effect, *b* — transverse effect.

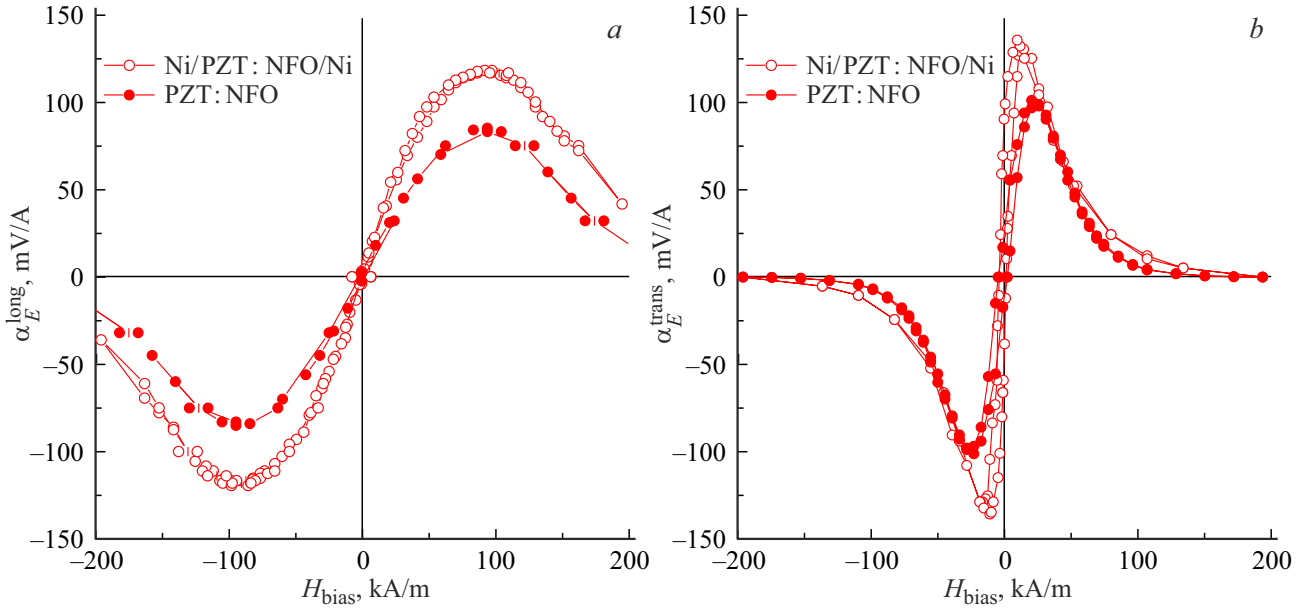

Figure 5. MEVC vs. bias field for PZT : NFO composite with composition 50 : 50% and For hybrid structures Ni/PZT : NFO/Ni with two layers of nickel 20 μm thick each: *a* — longitudinal effect, *b* — transverse effect.

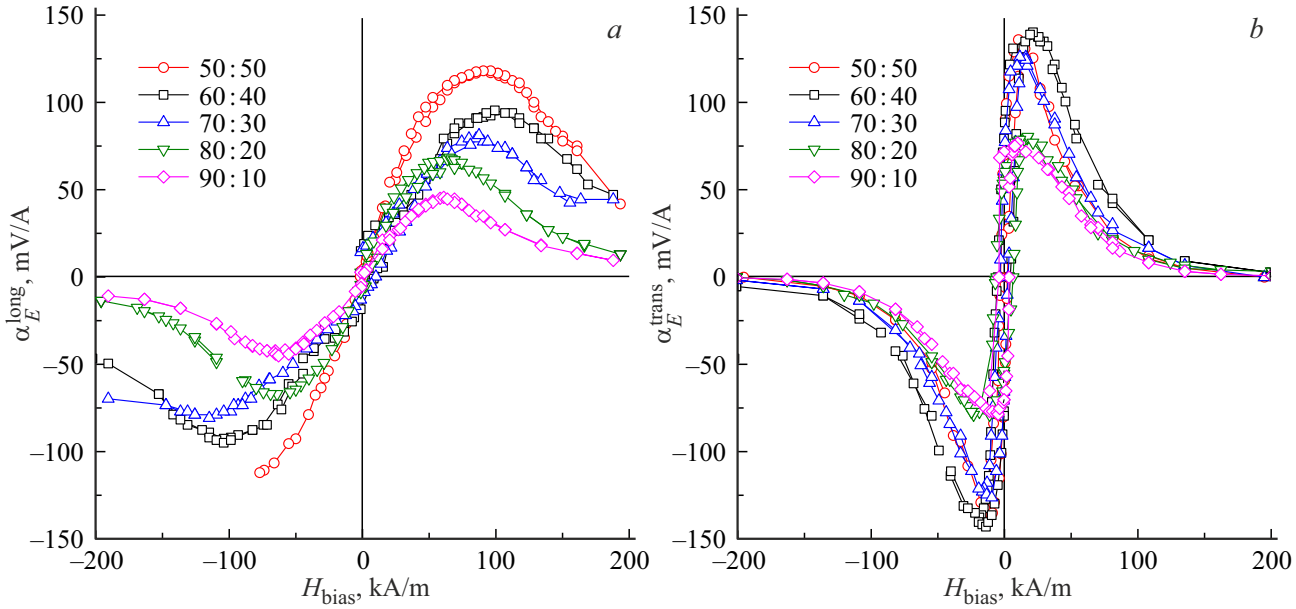

Figure 6. MEVC bias field for hybrid structure Ni/PZT : NFO/Ni with nickel layers 20 μm thick vs. composition of PZT : NFO composite: *a* — longitudinal effect, *b* — transverse effect.

deposition. As shown by the experimental results, additional layers lead to MEVC increasing with both longitudinal and transverse effects, and the magnitude of the effect depends on both the thickness of the applied layers and the percentage content of ferrite in the bulk PZT : NFO composite. Figure 5 shows the field dependences of MEVC with longitudinal and transverse effects for the ME-composite PZT : NFO of composition 50 : 50% and with nickel layers 20 μm thick each deposited on it on both sides.

As can be seen from Figure 5, for the hybrid structure the magnitude of the effect at the maximum is almost by one and a half times greater than the magnitude of the effect in PZT : NFO composite for both longitudinal and transverse effects, and the field value at which the maximum of the effect occurs, shifts to the region of weaker fields.

The experimental results showed that the magnitude of the effect for the hybrid structure depends both on the composition of PZT : NFO composite and on the thickness

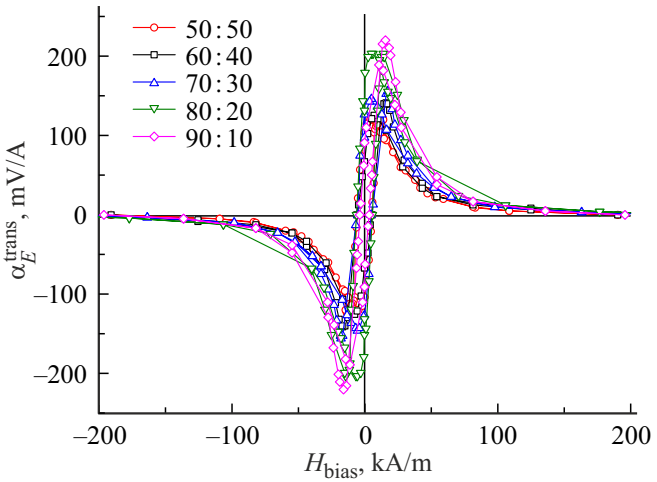

Figure 7. MEVC magnetization field for hybrid structure Ni/PZT:NFO/Ni with nickel layers 100 μm thick vs. composition of PZT:NFO composite at transverse effect.

of the additional magnetostrictive layers applied. Figure 6 shows the dependence of MEVC on the composition of PZT:NFO composite for Ni/PZT:NFO/Ni hybrid structure with nickel layer 20 μm thick each.

Data from the experimental study of linear low-frequency MEVC during transverse field orientation for hybrid structures with nickel thickness 100 μm are presented in Figure 7.

From a comparison of the graphs presented in Figure 6, *b* and Figure 7 it follows that increase in Ni thickness from 20 to 100 μm leads to a redistribution of the maxima of the ME coefficient. In this case, the maximum value is observed in structures with PZT:NFO concentration in the ratio 90:10%, and the minimum in the structure with 50:50%. The results obtained can be explained on the basis of model based on the joint solution of a system of equations for each of the phases included in the hybrid structure. Carrying out calculations similar to those in [33] for MEVC hybrid structure caused by planar oscillations, we obtain the following expression:

$$\alpha_{E,\text{long}} = \frac{Y^{ME} d_{31}^{ME}}{\varepsilon_{33} Y t} \times \frac{\left[Y^{ME} t^{ME} (q_{11}^{ME} + q_{12}^{ME}) + 2Y^{\text{Ni}} t^{\text{Ni}} (q_{11}^{\text{Ni}} + q_{12}^{\text{Ni}})\right]}{\left[1 - 2k_p^2 (1 - Y^{ME} t^{ME} / \bar{Y} t)\right]}. \quad (2)$$

Here Y^{ME}, Y^{Ni}, t^{ME}, t^{Ni} — Young's moduli and thickness of PZT:NFO composite and Ni respectively, d_{31}^{ME}, q_{1i}^{ME} and ε_{33} — effective values of piezoelectric moduli and dielectric permeability of composite, q_{1i}^{Ni} — value of piezomagnetic modulus module of Ni, k_p^2 — square of electromechanical coupling coefficient, $t = t^{ME} + 2t^{\text{Ni}}$ — thickness of hybrid structure, $\bar{Y} = (Y^{ME} t^{ME} + 2Y^{\text{Ni}} t^{\text{Ni}})/t$ — average value of Young's modulus of structure.

From expression (2) it follows that at small thicknesses of nickel $t^{\text{Ni}} \ll t^{ME}$ the decisive contribution to the magnitude of the effect will be made by the first term in square brackets in the numerator of equation (2), therefore the dependence of MEVC of the hybrid structure on the concentration ratio PZT:NFO will repeat the concentration dependence of the bulk NFO:PZT composite. The only difference will be that the contribution of Ni is proportional not only to the thickness of the layer, but also to the value of the effective piezoelectric modulus of the composite d_{31}^{ME}, which decreases with increase in percentage content of ferrite, so the maximum dependence for the hybrid structure falls on the composition 60:40, and not the composition 50:50, as for the bulk NFO:PZT composite. Besides, the presence of ferromagnetic Ni layer leads to increase in the magnetic field induction acting on the bulk NFO:PZT composite, as a result of which the maximum MEVC value shifts to the region of lower values of the bias field.

With increase in the Ni layer thickness, the contribution of the second term in square brackets in the numerator of equation (2) to the magnitude of the effect will be decisive, therefore the maximum MEVC value will be observed in the hybrid structure with the maximum effective value of the piezoelectric modulus d_{31}^{ME}, i.e. in the structure with composition 90:10. However, the first term also contributes to the magnitude of the effect, as a result of which the dependence of MEVC on the composite composition is observed.

Figure 8 shows the results of studies of the field dependence of MEVC for hybrid structures with alternating layers Ni/Co/Ni.

As follows from Figure 8, in the hybrid structure consisting of alternating layers Ni/Co/Ni (20/40/20 μm) the magnitude of the effect is less than in hybrid structure consisting of deposited layers of nickel (100 μm). Besides, the expected increase in the magnitude of the effect at zero bias field associated with the presence of the

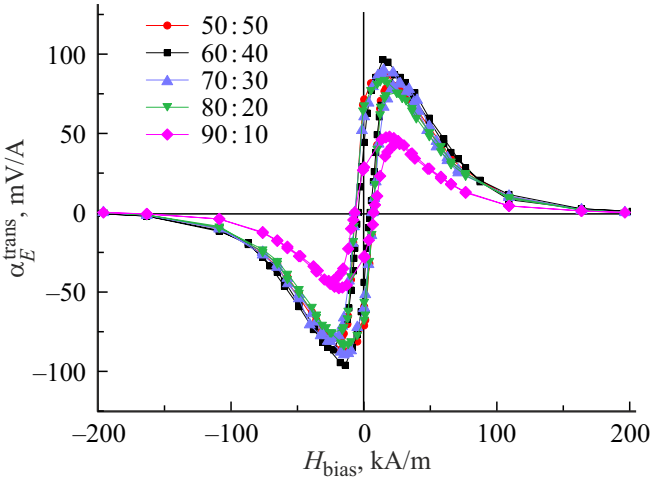

Figure 8. MEVC bias field for hybrid structure Ni/Co/Ni/PZT:NFO/Ni/Co/Ni with layers 20/40/20 μm thick vs. composition of PZT:NFO composite at transverse effect.

magnetization gradient was not observed. Thus, in the hybrid structure with alternating Ni/Co/Ni layers at zero bias field, the maximum value of the effect was 71 mV/A, while in the structure with Ni layers the maximum value of the effect at $H_{\text{bias}} = 0$ was 131 mV/A. From this we can conclude that the „self-bias“ effect is not associated with the presence of the magnetization gradient, but is associated, as shown in the papers [34,35], with the presence of residual magnetization.

4. Conclusion

As a result of the studies it was established that the use of additional layers of ferromagnetic metals leads to increase in the ME interaction of the hybrid structure compared to the bulk NFO : PZT composite. This enhancement is observed with both longitudinal and transverse effects. It is due to the fact that the presence of additional magnetostrictive layers leads to increase in deformations of the bulk ME composite, which leads to increase in MEVC. Besides, the presence of additional ferromagnetic layers leads to the increase in the magnetic field in the bulk composite, as a result of which the maximum MEVC value is achieved at a lower magnetization field compared to the bulk PZT : NFO composite, and the magnitude of the longitudinal effect becomes comparable in value with transverse effect.

The creation of structures with alternating layers Ni/Co/Ni having the magnetization gradient did not lead to the expected effect of MEVC increasing at zero bias field, compared to the hybrid structure with a nickel coating. This allows us to assume that the effect of „self-bias“ i. e. the occurrence of ME effect at zero bias field is not associated with the presence of magnetization gradient, but is due to residual magnetization.

As it was shown, the presence of metal coatings with magnetostrictive properties makes it possible to increase MEVC, and leads to a shift in the maximum value of the coefficient to the region of lower magnetic fields. This makes it possible to increase the sensitivity of such structures to changes in the magnetic field, which is promising for practical applications.

Funding

The paper was supported by the Belarusian Fundamental Scientific Research Foundation under grant F20MC–006. The study was carried out under grant from the Russian Science Foundation No. 22-19-00763, https://rscf.ru/project/22-19-00763/ at Yaroslav-the Wise Novgorod State University.

Conflict of interest

The authors declare that they have no conflict of interest.

References

[1] A.A. Bukharaev, A.K. Zvezdin, A.P. Pyatakov, Yu.K. Fetisov. UFN **188**, *12*, 1288 (2018). (in Russian)
[2] M. Bichurin, R. Petrov, O. Sokolov, V. Leontiev, V. Kuts, D. Kiselev, Y. Wang. Sensors **21**, 6232 (2021).
[3] T. Deng, Z. Chen, W. Di, R. Chen, Y. Wang, L. Lu, H. Luo, T. Han, J. Jiao, B. Fang. Smart Mater. Struct. **30**, 085005 (2021).
[4] J. Gao, Z. Jiang, S. Zhang, Z. Mao, Y. Shen, Z. Chu. Actuators **10**, 109 (20210).
[5] V. Annapureddy, H. Palneedi, W.-H. Yoon, D.-S. Park, J.-J. Choi, B.-D. Hahn, C.-W. Ahn, J.-W. Kim, D.-Y. Jeong, J.A. Ryu. Sensors Actuators A **260**, *15*, 206 (2017).
[6] D. Viehland, M. Wuttig, J. McCord, E. Quandt. MRS Bull. **3**, 834 (2018).
[7] V.N. Serov, D.V. Chashin, L.Y. Fetisov, Y.K. Fetisov, A.A. Berzin. J. IEEE Sensors **18**, *20*, 8256 (2018).
[8] D.A. Burdin, D.V. Chashin, N.A. Ekonomov, Y.K. Fetisov, A.A. Stashkevich. JMMM **405**, 244 (2016).
[9] V. Annapureddy, H. Palneedi, G.-T. Hwang, M. Peddigari, D.-Y. Jeong, W.-H. Yoon, K.-H. Kim, J. Ryu. Sustainable Energy Fuels **1**, 2039 (2017).
[10] C. M. Leung, X. Zhuang, D. Friedrichs, J. Li, R. W. Erickson, V. Laletin, M. Popov, G. Srinivasan, D. Viehland. Appl. Phys. Lett. **111**, 122904 (2017).
[11] J. Zhang, W. Zhu, D.A. Filippov, W. He, D. Chen, K. Li, S. Geng, Q. Zhang, L. Jiang, L. Cao, R. Timilsina, G. Srinivasan. Rev. Sci. Instrum. **90**, 015004 (2019).
[12] Y. Yan, L. D. Geng, L. Zhang, X. Gao, S. Gollapudi, H.-C. Song, S. Dong, M. Sanghadasa, K. Ngo, Y.U. Wang, S. Priya. Sci. Rep. **7**, 16008 (2017).
[13] J. Yu, L. Bai, R. Gao. Proc. Appl. Ceram. **14**, *4*, 336 (2020).
[14] X. Qin, R. Xu, H. Wu, G. Rongli, Z. Wang, G. Chen, C. Fu, X. Deng, W. Cai. Proc. Appl. Ceram. **13**, *4*, 349 (2019).
[15] R. Elshater, A.S. Atlam, M.K. Elnimr, S.T. Assar, D. Tishkevich, T. Zubar; S. Trukhanov, A.V. Trukhanov, D. Zhou, M. Darwish. Mater. Sci. Eng. B **286**, *10*, 116025 (2022).
[16] Y. Fetisov, D. Chashin, D. Saveliev, L. Fetisov, M. Shamonin. Materials **12**, *19*, 3228 (2019).
[17] G. Schileo, C. Pascual-Gonzalez, M. Alguero, I.M. Reaney, P. Postolache, L. Mitoseriu, K. Reichmann, M. Venet, A. Feteira. J. Eur. Ceram. Soc. **38**, *4*, 1473 (2017).
[18] G. Wu, R. Zhang. JETPLet **48**, *24*, 3 (2022).
[19] S. Saha, R.P. Singh, Y. Liu, A.B. Swain, A. Kumar, V. Subramanian, A. Arockiarajan, G. Srinivasan, R. Ranjan. Phys. Rev. B **103**, L140106 (2021).
[20] M. Popov, Y. Liu, V.L. Safonov, I.V. Zavislyak, V. Moiseienko, P. Zhou, G. Srinivasan. Phys. Rev. Appl. **14**, *3*, 1 (2020).
[21] L.Y. Fetisov, D.V. Chashin, D.V. Saveliev, M.S. Afanas'ev, I.D. Simonov-Emel'yanov, M.M. Vopson, Y.K. Fetisov. JMMM **485**, *9*, 251 (2019).
[22] S.K. Chacko, B. Raneesh. J. Mater. Sci. **58**, *3*, 1158 (2023).
[23] G. Schileo, C. Pascual-Gonzalez, M. Alguero, I.M. Reaney, P. Postolache, L. Mitoseriu, K. Reichmann, M. Venet, A. Feteira. J. Eur. Ceram. Soc. **38**, *4*, 1473 (2018)
[24] J. Zhang, B. Ge, Q. Zhang, J. Wu, J. Tao, J. Chen, L. Jiang, L. Cao. IEEE Transact. Magn. **58**, *2*, 1 (2022).
[25] B. Ge, J. Zhang, Q. Zhang, D.A. Filippov, J. Wu, J. Tao, J. Chen, L. Jiang, L. Cao, G. Srinivasan. JMMM **564**, *12*, 170115 (2022).

[26] Y. Wang, D. Gray, D. Berry, J. Gao, M. Li, J. Li, D. Viehland. Adv. Mater. **23**, 4111 (2011).
[27] V. Laletin, N. Poddubnaya, D. Filippov. AIP Conf. Proc. **2486**, 030021 (2022).
[28] D.V. Chashin, Y.K. Fetisov, K.E. Kamentsev, G. Srinivasan. Appl. Phys. Lett. **92**, 102511 (2008).
[29] S.R.Murphy, T.S. Rao. Phys. Status Solidi A **90**, 631 (1985).
[30] M.I. Bichurin, R.V. Petrov, V.S. Leontiev, O.V. Sokolov, A.V. Turutin, V.V. Kuts, I.V. Kubasov, A.M. Kislyuk, A.A. Temirov, M.D. Malinkovich, Y.N. Parkhomenko. Sensors **20**, 7142 (2020).
[31] D.A. Filippov V.M. Laletin, G. Srinivasan. ZhTF **82**, *1*, 47 (2012). (in Russian).
[32] M.I. Bichurin, V.M. Petrov, G. Srinivasan. Phys. Rev. **68**, 054402 (2003).
[33] D.A. Filippov, T.A. Galkina, I.N. Manicheva. ZhTF **93**, *2*, 230 (2023). (in Russian)
[34] J. Zhang, D.K. Li, D.A. Filippov, B. Ge, Q. Zhang, X. Hang, L. Cao, G. Srinivasan. AIP Advances **9**, 035137 (2019).
[35] Y. Liu, J. Zhang, P. Zhou, C. Dong, X. Liang, W. Zhang, T. Zhang, N.X. Sun, D. Filippov, G. Srinivasan. J. Appl. Phys. **126**, 114102 (2019).

Translated by I.Mazurov